NOTES

Magnetic Resonance in Medicine 60:727–731 (2008)

In Vivo ^{1}H NMR Measurement of Glycine in Rat Brain at 9.4 T at Short Echo Time

Giulio Gambarota,* Lijing Xin, Chiara Perazzolo, Ingrid Kohler, Vladimír Mlynárik, and Rolf Gruetter

Glycine is an amino acid present in mammalian brain, where it acts as an inhibitory and excitatory neurotransmitter. The two detectable protons of glycine give rise to a singlet at 3.55 ppm that overlaps with the more intense *myo*-inositol resonances, and its measurement has traditionally required specific editing efforts. The aim of the current study was to reduce the signal intensity of *myo*-inositol relative to that of glycine by exploiting the fast signal J-evolution of the *myo*-inositol spin system when using a single spin-echo localization method we recently introduced. Glycine was detected at TE = 20 ms with an average Cramér-Rao lower bound (CRLB) of 8.6% ± 1.5% in rat brain (*N* = 5), at 9.4 T. The concentration of glycine was determined using LCModel analysis at 1.1 ± 0.1 mM, in good agreement with biochemical measurements previously reported. We conclude that at high magnetic fields, glycine can be measured at a relatively short echo time (TE) without additional editing efforts. Magn Reson Med 60:727–731, 2008. © 2008 Wiley-Liss, Inc.

Key words: glycine; strongly coupled spin system; NMR spectroscopy; density matrix simulations; rat brain

Glycine is an amino acid present in mammalian brain, where it acts as an inhibitory and excitatory neurotransmitter (1). Because of its critical role in N-methyl-D-aspartic acid (NMDA) transmission, altered levels of glycine are involved in a number of pathologies. In particular, elevated levels of glycine have been observed in the brain tissues of hyperglycinemia patients and in tumors (2,3). In a number of studies, glycine has been administered to schizophrenia patients to improve the NMDA receptor function, with the result of a significant decrease in negative and cognitive symptoms (4,5). Given its importance in mediating the action of the major excitatory neurotransmitter glutamate, a direct measurement of brain glycine concentration is desirable. The noninvasive measurement of glycine in brain is hampered by the fact that its two-proton singlet resonance at 3.55 ppm overlaps with the resonances of *myo*-inositol, which is present in the brain at much higher concentrations. Not surprisingly, glycine detection has only been reported in the human brain, using long TE when glycine was elevated or using additional editing techniques, such as TE-averaged point-resolved spectroscopy (PRESS) or 2D J-PRESS (6,7). Despite the fact that animal studies are typically performed at high field strengths (≥7 T), where the substantial increase in SNR and spectral resolution could allow glycine detection without editing or TE-averaging, we are not aware of any such report to date.

At very short TE (~1–2 ms), multiplet resonances from coupled spin systems display virtually no dephasing induced by J-modulation. As TE increases, a loss of signal intensity occurs due to J-modulation. In particular, when using a single spin echo coherence generation at high field, *myo*-inositol undergoes rapid J-modulation due to its large J-coupling of ~10 Hz. In this study we sought to reduce the signal intensity of *myo*-inositol relative to that of glycine by exploiting its J-evolution when using a single spin-echo coherence excitation. We therefore hypothesized that it is feasible to quantify glycine at 9.4 T in rat brain in vivo, using a spin-echo full intensity acquired localization (SPECIAL) scheme (8) at short echo times (TEs).

MATERIALS AND METHODS

Theory: Overlap of Glycine With *myo*-Inositol

Myo-inositol consists of six CH groups that generate a complex spectral pattern in the ^{1}H MR spectrum and can be modeled as an AM_2N_2P spin system. The M protons resonate at 3.52 ppm (M_2), the N resonates at 3.61 ppm (N_2), and the A and P protons resonate at 4.05 and 3.27 ppm, respectively (9). In contrast, the two protons of glycine constitute a singlet at 3.55 ppm, which overlaps with the resonances M and N of *myo*-inositol. The J-coupling constant between the M_2 and N_2 protons is J is 9.99 Hz. At 9.4 T, the ratio of the chemical shift difference to the coupling constant for the MN coupling is ~3; as a consequence, the M and N protons are strongly coupled. As TE increases, the J-coupling introduces a dephasing in the M_2 resonance that can be exploited for detecting the glycine singlet.

To evaluate the potential choice of TE that allows one to reduce the signal intensity of *myo*-inositol relative to that of glycine, the spectrum of *myo*-inositol was simulated as a function of TE, for a single spin-echo excitation, using quantum-mechanics simulations based on the density matrix formalism (10,11). The density matrix operator $\sigma(t)$ for the spin-echo excitation was written as:

$$\sigma(t) = R^{-}F_zR^{+}, \quad [1]$$

Laboratory of Functional and Metabolic Imaging, École Polytechnique Fédérale de Lausanne, Lausanne, Switzerland.

Grant sponsor: Centre d'Imagerie BioMédicale of the UNIL, UNIGE, HUG, CHUV, EPFL, Leenaards Foundation, and Jeantet Foundation; Grant sponsor: Swiss National Science Foundation; Grant number: 3100A0-116220.

*Correspondence to: Giulio Gambarota, Ph.D., Swiss Federal Institute of Technology Lausanne (EPFL), SB-LIFMET, CH F0 626, Station 6, CH-1015 Lausanne, Switzerland. E-mail: giulio.gambarota@epfl.ch

Received 11 August 2007; revised 22 April 2008; accepted 23 April 2008.

DOI 10.1002/mrm.21695

Published online in Wiley InterScience (www.interscience.wiley.com).

where $R^- = e^{-i\,t\,H}\,e^{-i\,TE/2\,H}\,e^{-i\,\pi\,F_y}\,e^{-i\,TE/2\,H}\,e^{-i\pi/2\,F_x}$, and $R^+ = e^{i\,\pi/2\,F_x}\,e^{i\,TE/2\,H}\,e^{i\,\pi\,F_y}\,e^{i\,TE/2\,H}\,e^{i\,t\,H}$, with H being the Hamiltonian for the coupled spin system of *myo*-inositol, and F_z, F_x, and F_y being the z, x, and y magnetic moment operators, respectively. The transverse magnetization at time t was found by calculating the trace of the product of the density matrix operator with the transverse magnetic moment operator F_+, where $F_+ = F_x + i\,F_y$ (11). The time signal was generated from F_+ for 4096 points over an acquisition time of 1.024 s. Spectra were obtained by fast Fourier transform of the calculated time signal, with a line-broadening factor applied to generate singlet linewidths that matched those observed in vivo.

MR Experiments

Experiments were performed on five healthy male Sprague Dawley rats (320 ± 60 g, mean ± standard deviation [SD]) that were anesthetized by 1.5% to 2.0% isoflurane using a nose mask. Body temperature was maintained at 37.5°C ± 1°C with a circulating warm-water pad. All procedures were performed in accordance with local and federal guidelines and approved by the local ethics committee. Measurements were performed on a Varian INOVA spectrometer (Varian, Palo Alto, CA, USA) interfaced to an actively shielded 9.4T/31-cm magnet (Magnex Scientific, Abingdon, UK) with actively shielded gradients (400 mT/m in 120 μs, 12-cm inner diameter). An in-house-built quadrature surface coil with two 14-mm-diameter single loops was used as a transmitter/receiver. Gradient-echo multislice images were acquired for anatomical localization of the brain, to select a voxel of interest (VOI) of 2.5 × 5 × 5 mm^3 centered in the hippocampus. First- and second-order shims were adjusted for the selected VOI using an EPI version of FASTMAP (12), resulting in a water linewidth of 12–15 Hz. Spectra were acquired at TE = 2.8 and 20 ms with the SPECIAL sequence (TR = 4000 ms, spectral width = 5000 Hz, acquired complex points = 4096). The SPECIAL implementation consisted of a spin-echo sequence with 0.5 ms 90° and 180° asymmetric slice-selective pulses. Signal localization in the third dimension was achieved by a 1D image-selected in vivo spectroscopy (ISIS) approach (13), implemented with a 2-ms slice-selective adiabatic full-passage pulse applied on alternate scans. Water signal suppression and outer volume suppression was achieved as described in Ref 8. For each experiment, a total of 160 scans were acquired in 10 separate blocks of 16 scans each. Fourier transformation and B_0 shift correction were performed prior to summation of the 10 spectra. To analyze the dependence of the Cramér-Rao lower bound (CRLB) on the signal-to-noise ratio (SNR, as estimated by the LCModel), six spectra were generated from each experiment by averaging 16, 32, 64, 96, 128, and 160 scans, respectively. Metabolite concentrations and CRLBs were determined by spectral data analysis performed with LCModel 6.1 (14) using total creatine as an internal reference (8 mM) for quantitation (15). In vitro MRS experiments were performed on a pH-balanced (pH = 7.0) phantom containing 50 mM *myo*-inositol and 8.3 mM glycine, to approximately mimic the in vivo concentration ratio. Spectra were acquired at the same TEs as in the in vivo measurements. During the experiments, the temperature of the phantom was kept at 37°C.

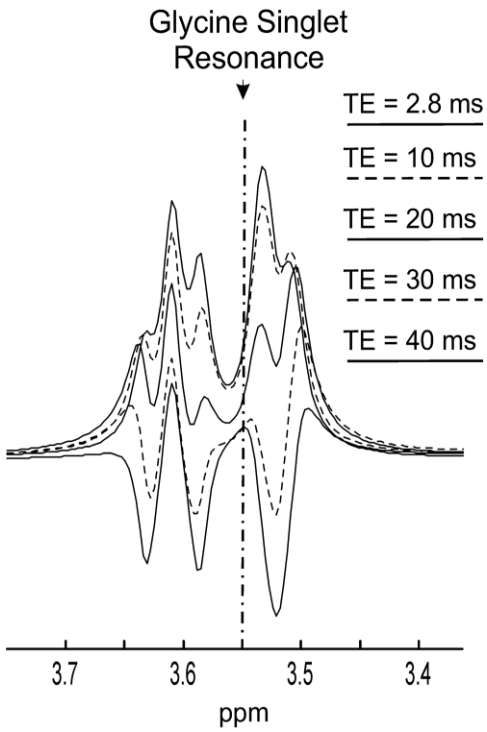

FIG. 1. Simulated proton MR spectra of the *myo*-inositol resonances in the 3.4–3.7 ppm region, at TE = 2.8, 10, 20, 30, and 40 ms, from top to bottom, using SPECIAL excitation at 9.4 T. At TE = 20 ms, the *myo*-inositol signal substantially decreases due to J-modulation, in particular at the resonance frequency of the glycine singlet (3.55 ppm). At TEs longer than 20 ms, the *myo*-inositol resonances adjacent to the glycine singlet display opposite phase.

RESULTS

Quantum-mechanics simulations based on the density matrix formalism provided the spectral shape of *myo*-inositol at different TEs. When using single spin-echo coherence generation, the *myo*-inositol resonances in the 3.4–3.7 ppm region underwent rapid J-modulation at 9.4 T, displaying opposite phase already at TE greater than 20 ms (Fig. 1). At short TE, the signal intensity of the combined spectrum (*myo*-inositol + glycine) differed only slightly from that of *myo*-inositol (Fig. 2a). Overall, the effect of the glycine peak on the whole spectrum was mostly to slightly broaden the M_2 resonance of *myo*-inositol, resulting in a very small increase of the M_2 resonance height. At a TE of 20 ms, J-evolution already caused a substantial effect on the signal intensity of *myo*-inositol resonances. In particular, the signal intensity of the M_2 protons showed a ~50% decrease due to J-modulation, and as a result the glycine resonance was now comparable to the M_2 resonance (Fig. 2b). At this TE, the combined spectrum was visually clearly discernible from that of *myo*-inositol alone. More specifically, the peak height at ~3.55 ppm (which consists of the M_2 resonance of *myo*-inositol and glycine) approached the height of the M_2 resonance at ~3.51 ppm, while in the *myo*-inositol spectrum the peak at 3.55 ppm was reduced compared to the peak at 3.51 ppm. The spectral pattern of the *myo*-inositol resonances measured in vitro was in excellent agreement with the spectral pattern

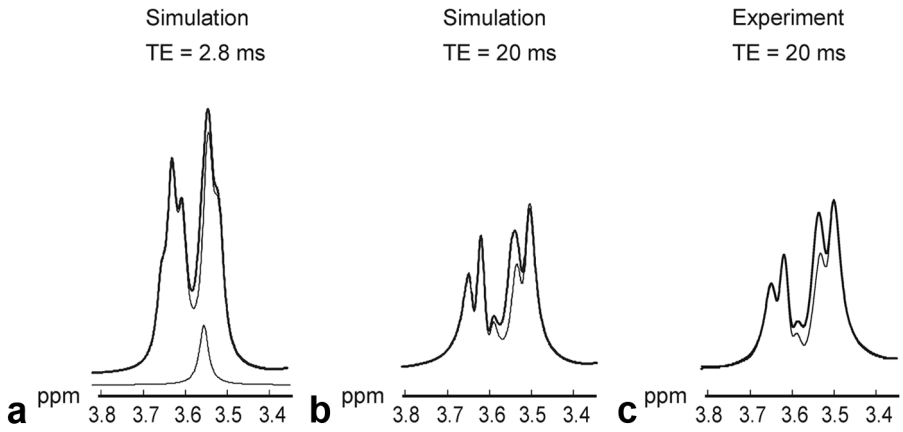

FIG. 2. Simulated (**a** and **b**) and in vitro (**c**) proton MR spectra of *myo*-inositol (thin line) and *myo*-inositol + glycine (thick line) using SPECIAL excitation at 9.4 T. For clarity, the glycine singlet is shown only in the left spectrum. At TE = 2.8 ms, the *myo*-inositol + glycine spectrum differs only slightly from the *myo*-inositol spectrum. At TE = 20 ms, the *myo*-inositol signal substantially decreases due to J-modulation. In the simulated spectra, the relaxation effect is not taken into account. The in vitro spectra display the same spectral pattern of the *myo*-inositol resonances as the simulated spectra.

of simulated spectra, reproducing the characteristic asymmetry between the height of the 3.55 and 3.51 ppm peaks and its reduction by the presence of glycine (Fig. 2c).

At TE of 20 ms, the fit of the in vivo spectrum to a basis set that did not include the glycine peak yielded a discernible fit residual with positive amplitude at 3.55 ppm (Fig. 3a, middle trace). Upon inclusion of the glycine peak, the residual at 3.55 ppm was minimized to the noise level (Fig. 3a, bottom trace). The improvement of the fit is further indicated by the arrow at the resonance frequency of glycine in Fig. 3b. Glycine concentration was 1.1 ± 0.1 mM with an average CRLB of 8.6% ± 1.5% (Table 1). For the very short TE spectrum, the mean CRLB of glycine was 33%.

The quantification of metabolites other than glycine revealed that at a TE of 20 ms, the CRLB of strongly represented metabolites increased only slightly with respect to the values obtained at the TE of 2.8 ms. For example, the average CRLB of glutamate was 1.4% ± 0.5% and 2.2% ± 0.4%, at TE of 2.8 and 20 ms, respectively, corresponding to a CRLB increase, expressed in absolute value, of less than 1%. The increase in CRLB was 1% for *myo*-inositol, creatine, and phosphocreatine; 2% for taurine; and 3% for glutamine. There was no increase for N-acetylaspartate.

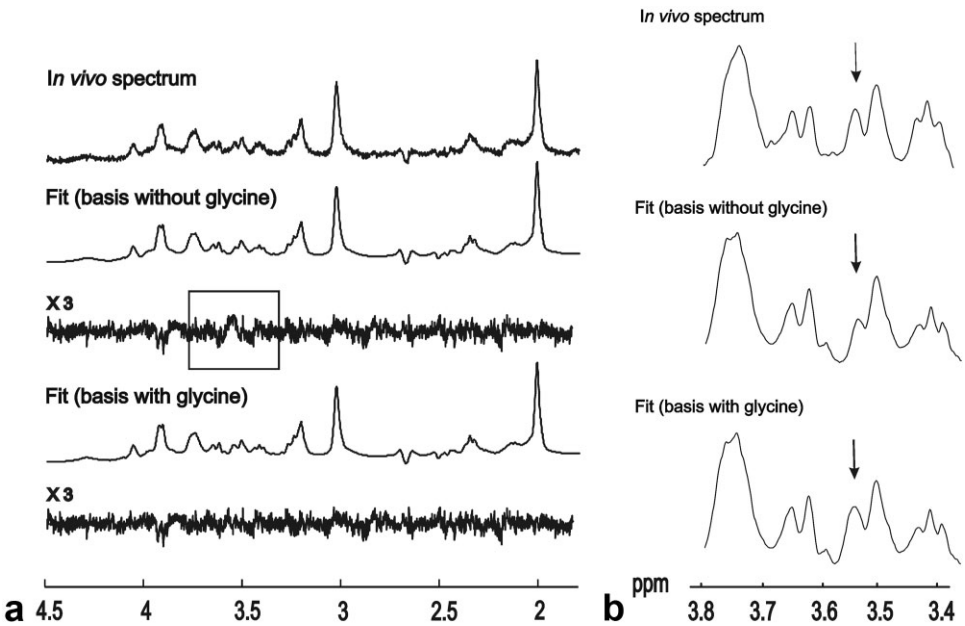

FIG. 3. **a:** In vivo proton MR spectrum (TE = 20 ms) and LCModel fits. Below each fit the residual (enlarged 3×) is shown. The box highlights the residual at the resonance frequency of the glycine singlet. **b:** Zoom in the region at 3.55 ppm of an in vivo proton MR spectrum (top) and LCModel fits without (middle) and with (bottom) glycine in the basis set. The in vivo spectrum (top) was line-broadened to match the fit (middle and bottom) obtained from the LCModel output. The arrow indicates the 3.55 ppm resonance frequency.

Table 1
Glycine and *Myo*-Inositol Concentration, CRLB of Glycine and Correlation Coefficient Between Glycine and *Myo*-Inositol Measured in Five Rats at TE = 20 ms

Rat	Gly (mM)	*Myo*-Ins (mM)	Gly CRLB (%)	Correlation coefficient
#1	1.13	5.49	8	−0.009
#2	1.04	5.74	11	−0.003
#3	1.00	4.66	8	0.066
#4	1.25	4.80	7	0.127
#5	1.20	5.54	9	0.029

Gly = glycine, *Myo*-ins = *myo*-inositol.

For all the aforementioned metabolites, the values of the CRLB remained below 10%. Furthermore, for the strongly represented metabolites, the concentration estimated at TE = 20 ms was similar to that estimated at TE = 2.8 ms. In particular, at TE = 2.8 and 20 ms, the concentration of glutamate was 9.9 ± 0.7 and 10.2 ± 0.4, of glutamine 2.8 ± 0.8 and 3.2 ± 0.2, of *myo*-inositol 5.3 ± 0.6 and 5.2 ± 0.5, of taurine 5.7 ± 0.7 and 5.4 ± 0.5, and of N-acetylaspartate 9.0 ± 0.5 and 8.8 ± 0.5 (mean ± SD, $N = 5$), respectively. At TE of 20 ms, the CRLB of less well represented metabolites, such as glucose, ascorbate, and γ-aminobutyric acid (GABA), for example, increased more substantially and to different degrees. Other less well-represented metabolites, such as alanine and aspartate, were not consistently detected.

To evaluate the dependence of the CRLB on the SNR, data analysis of spectra containing an increasing number of scans was performed. At the SNR of 20 (measured for the N-acetylaspartate singlet), the CRLB of glycine was below 15%. For increasing SNR, the CRLB decreased, reaching ~8% at an SNR of 32 (Fig. 4).

DISCUSSION

The glycine resonance, being a singlet at 3.55 ppm that is overlapped by the more intense *myo*-inositol resonances, cannot be directly edited as has been used for coupled spin systems such as GABA (16), but requires approaches that minimize the signal contribution from *myo*-inositol. In the present study, we show that with a TE of 20 ms it is possible to reliably detect glycine at 9.4 T in rat brain in vivo. With respect to the choice of TE = 20 ms, this is a TE at which the amplitude of the M_2 resonance is sufficiently reduced to allow for glycine detection. Compared to longer TEs, where the M_2 resonance amplitude is reduced as well, this TE yields minimal T_2 losses. Furthermore, at TE greater than 20 ms, the *myo*-inositol lineshape has an opposite phase, which could lead to partial cancellation with the singlet of glycine. It should be noted that these arguments apply only to the case of single spin-echo coherence excitation. The single spin-echo excitation yields a decrease of the *myo*-inositol signal intensity that is faster than that generated by the double spin-echo excitation, as implemented in the commonly used PRESS. In PRESS, at the relatively short TE of 20 ms, the closely-spaced 180° pulses partially quench the J-modulated losses in coupled spin systems (17), resulting in a signal dephasing that is smaller than that induced by a single spin-echo excitation. As a consequence, TEs longer than 20 ms may be advantageous for glycine detection with a PRESS sequence. Other approaches designed to exploit the J-modulation of the coupled resonance, such as TE-averaged PRESS, may not be favorable at very high field strengths, since the shorter T_2 relaxation times of metabolites could result in an incomplete cancellation of the outer bands of multiplets.

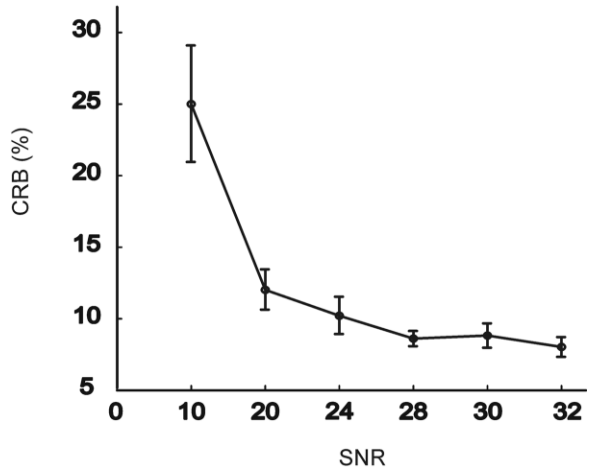

FIG. 4. CRLB as a function of the SNR. Glycine concentration was quantified with CRLB below 10% at SNR greater than 24.

In ^{1}H MR spectroscopy, the CRLB provides a measure of the reliability of metabolite concentration measurements, which in turn relies on the quality of the spectrum, in particular the linewidth and SNR. Here we have provided a quantitative analysis of the SNR needed to achieve a CRLB for glycine quantitation below 10%. Even at an SNR value of ~20, the CRLB was well below 20%, supporting the notion that the proposed approach for measuring glycine provides a high reliability. The low correlation coefficient between glycine and *myo*-inositol, as estimated from the covariance matrix by the LCModel, suggests minimal covariance effects at TE = 20 ms. The value of glycine concentration measured in the current study is in good agreement with previously reported biochemical measurements, where average values of concentration in adult rats range from 1.2 to 1.6 mM (18–20). With respect to the value of glycine concentration reported in human brain, our result is in good agreement with the value reported by Schulte and Boesiger (7) (Gly/Cr ratio = 0.123, CRLB = 12% ± 3%), measured at 3 T with 2D J-PRESS. On the other hand, both our values and those of Schulte and Boesiger (7) are smaller than the value measured at 4 T

with TE-averaged PRESS by Prescot et al. (6) (Gly*/Cr ratio ~ 0.03, CRLB = 16% ± 2%, where the Gly* consists of the glycine peak with a partial contribution from the *myo*-inositol resonance). The methodology employed in the current study could also be extended to measurements of glycine in human brain, at field strengths (7 T, for instance) where sufficient spectral dispersion allows for clear separation of the M_2 and N_2 *myo*-inositol resonances. On the other hand, since the J-modulated signal dephasing in strongly coupled spin systems is slower with decreasing field strength, a TE longer than 20 ms might be favorable at 7 T to minimize the amplitude of the M_2 resonance of *myo*-inositol.

In animal models, several metabolites can be reliably measured with ^{1}H MR spectroscopy. The highest number of metabolites is typically observed when measurements are performed at very high field (≥7 T) and at very short TE (~1–2 ms) (15). In the current study, glycine was not consistently detected in the spectra at TE of 2.8 m, in line with previous studies in animal models performed at very short TE (15). The increase of TE to 20 ms, which results in glycine detection, yields only a minor increase in the CRLB of strongly represented metabolites. On the other hand, less well-represented metabolites suffer to different degrees from the extended TE of 20 ms, reducing the ability to measure the full neurochemical profile. This can, however, still be accomplished by an additional measurement at very short TE.

The J-modulation of the coupled resonance signals measured experimentally was in excellent agreement with the quantum-mechanics simulations, as demonstrated by the good agreement between the simulated spectra and in vitro and in vivo results. Over the last two decades, many studies of the TE dependence of metabolite resonances have been performed to optimize metabolite detection at the field strength of clinical MR scanners. On the other hand, less attention has been paid to the TE dependence of metabolite resonances at very high field. The results of this study show that also at high field strengths, spin simulations are an important tool to aid in the choice of sequence parameters.

CONCLUSIONS

In the present study we show that it is possible to quantify glycine at 9.4 T in rat brain in vivo, at a short TE of 20 ms, without 2D spectroscopy or editing methods such as TE-averaging when using single spin echo coherence generation. This provides an experimentally simple approach that requires only a judicious choice of TE.

REFERENCES

1. Betz H, Laube B. Glycine receptors: recent insights into their structural organization and functional diversity. J Neurochem 2006;97:1600–1610.
2. Huisman TA, Thiel T, Steinmann B, Zeilinger G, Martin E. Proton magnetic resonance spectroscopy of the brain of a neonate with nonketotic hyperglycinemia: in vivo-in vitro (ex vivo) correlation. Eur Radiol 2002;12:858–861.
3. Kinoshita Y, Kajiwara H, Yokota A, Koga Y. Proton magnetic resonance spectroscopy of brain tumors: an in vitro study. Neurosurgery 1994;35:606–613; discussion 613–604.
4. Heresco-Levy U, Ermilov M, Lichtenberg P, Bar G, Javitt DC. High-dose glycine added to olanzapine and risperidone for the treatment of schizophrenia. Biol Psychiatry 2004;55:165–171.
5. Waziri R. Glycine therapy of schizophrenia. Biol Psychiatry 1988;23:210–211.
6. Prescot AP, de BFB, Wang L, Brown J, Jensen JE, Kaufman MJ, Renshaw PF. In vivo detection of brain glycine with echo-time-averaged (1)H magnetic resonance spectroscopy at 4.0 T. Magn Reson Med 2006;55:681–686.
7. Schulte RF, Boesiger P. ProFit: two-dimensional prior-knowledge fitting of J-resolved spectra. NMR Biomed 2006;19:255–263.
8. Mlynarik V, Gambarota G, Frenkel H, Gruetter R. Localized short-echo-time proton MR spectroscopy with full signal-intensity acquisition. Magn Reson Med 2006;56:965–970.
9. Govindaraju V, Young K, Maudsley AA. Proton NMR chemical shifts and coupling constants for brain metabolites. NMR Biomed 2000;13:129–153.
10. Gambarota G, van der Graaf M, Klomp D, Mulkern RV, Heerschap A. Echo-time independent signal modulations using PRESS sequences: a new approach to spectral editing of strongly coupled AB spin systems. J Magn Reson 2005;177:299–306.
11. Mulkern RV, Bowers J. Density matrix calculations of AB spectra from multiple sequences: quantum mechanics meets in vivo spectroscopy. Concepts Magn Reson 1994;6:1–23.
12. Gruetter R, Tkac I. Field mapping without reference scan using asymmetric echo-planar techniques. Magn Reson Med 2000;43:319–323.
13. Ordidge RJ, Connelly A, Lohman JAB. Image-selected in vivo spectroscopy (ISIS)—a new technique for spatially selective NMR-spectroscopy. J Magn Reson 1986;66:283–294.
14. Provencher SW. Estimation of metabolite concentrations from localized in vivo proton NMR spectra. Magn Reson Med 1993;30:672–679.
15. Pfeuffer J, Tkac I, Provencher SW, Gruetter R. Toward an in vivo neurochemical profile: quantification of 18 metabolites in short-echo-time (1)H NMR spectra of the rat brain. J Magn Reson 1999;141:104–120.
16. Terpstra M, Ugurbil K, Gruetter R. Direct in vivo measurement of human cerebral GABA concentration using MEGA-editing at 7 Tesla. Magn Reson Med 2002;47:1009–1012.
17. Allerhand A. Analysis of Carr-Purcell spin-echo NMR experiments on multiple-spin systems. I. Effect of homonuclear coupling. J Chem Physics 1966;44:1–9.
18. Mandel P, Mark J. The influence of nitrogen deprivation on free amino acids in rat brain. J Neurochem 1965;12:987–992.
19. Davis JM, Himwich WA, Pederson VC. Hypoglycemia and developmental changes in free amino acids of rat brain. J Appl Physiol 1970;29:219–222.
20. Cutler RW, Dudzinski DS. Regional changes in amino acid content in developing rat brain. J Neurochem 1974;23:1005–1009.